Thermal stability of polystyrene-*b*-poly(ethylene/propylene) diblock copolymer micelles in paraffinic solvents

M. Schouten*, J. Dorrepaal and W. J. M. Stassen
Koninklijke/Shell-Laboratorium, Amsterdam (Shell Research BV), PO Box 3003, 1003 AA Amsterdam, The Netherlands

W. A. H. M. Vlak
Netherlands Energy Research Foundation ECN, PO Box 1, 1755 ZG Petten, The Netherlands

and K. Mortensen
Risø National Laboratory, PO Box 49, 4000-DK Roskilde, Denmark
(Received 13 December 1988; accepted 24 February 1989)

The micelles formed by a polystyrene-*b*-poly(ethylene/propylene) diblock copolymer in two paraffinic solvents have been investigated with small-angle neutron scattering. At room temperature, the micelles consist of a core composed of insoluble polystyrene blocks surrounded by a well solubilized layer of ethylene/propylene chains. At polymer concentrations as low as 0.5% by weight, these micelles interact strongly, resulting in a 'fluid-like' distribution of the micelles over the solution volume. For a 1% concentration in n-dodecane the degree of intermicellar interaction diminishes dramatically when the temperature is raised from 100 to 140°C. Above 100°C the micelles start to decrease in size gradually, their total number, however, remaining the same. In combination with nuclear magnetic resonance and viscometry, neutron scattering suggests that it is only at elevated temperatures that polymer molecules are able to leave the micelle and enter the solution as individual molecules. It is discussed how this explains the sharp viscosity drop of these polymer solutions around 80°C.

(Keywords: diblock copolymers; micelles; small-angle neutron scattering; thermal stability)

INTRODUCTION

The diblock copolymer polystyrene-*b*-poly(ethylene/propylene) (PS-PEP) is well known to form micelles in solvents that are selectively poor for one of the blocks of the polymer[1,2]. In a paraffinic solvent such as n-dodecane, which is a precipitant for the polystyrene (PS) diblock of the polymer, the micelles consist of a polystyrene core from which well solubilized poly(ethylene/propylene) (PEP) blocks protrude into the solution.

It has been reported by Mandema *et al.* that the viscosity of PS-PEP solutions in n-decane decreases dramatically with increasing temperature over a transition region approximately 30°C wide[3,4]. Although dependent on the precise molecular weight of the two blocks of the polymer, this transition region typically sets in at 80°C. For PS-PEP solutions in a non-selective solvent, i.e. a solvent in which both blocks of the polymer are soluble and in which the polymer is not expected to form micelles (at least not at the polymer concentrations discussed here, viz. 0.5 to 2% by weight (w/w)), such a drop in the viscosity of the solution has not been observed. From this it was concluded that most probably the decrease in the viscosity in n-decane results from the dissociation around 90°C of PS-PEP micelles into individual polymer molecules.

Further evidence for the dissociation of the PS-PEP micelles at elevated temperatures, although of an equally indirect nature, seems to be furnished by nuclear magnetic resonance (n.m.r.) studies of solutions of the polymer in perdeuterated n-octane[5]. From investigations of the proton n.m.r. line width as a function of temperature, it has been inferred that at room temperature the PS blocks in PS-PEP solutions are highly immobile. The mobility of the PS blocks gradually increases with temperature, until around 100°C it is comparable to that of the PS blocks in a PS-PEP solution in a non-selective solvent, containing individual polymer molecules only.

Small-angle X-ray scattering (SAXS) experiments have shown that the micelles formed by polystyrene–polybutadiene (PS–PB) diblock copolymers in n-tetradecane arrange into a spatially ordered, simple-cubic lattice at high concentration (>8% w/w)[6–8]. For temperatures above a *lattice disordering temperature*, T_d, the cubic ordering disappears whilst the micelles remain intact. This lattice disordering involves the change of the long-range cubic ordering into a more short-ranged 'fluid-like' ordering of the micelles. Above T_d, the yield stress exhibited by these solutions vanishes, demonstrating that the rheological behaviour of the PS–PB solutions is intimately related with the tendency of the micelles to form a spatially organized structure. Below 8% w/w polymer concentration no organized structure has been observed for this system.

Recent small-angle neutron scattering (SANS) studies of a PS–PEP polymer in n-dodecane at room temperature

* Present address: Shell Internationale Petroleum Maatschappij B.V., PO Box 162, 2501 AN The Hague, The Netherlands

0032-3861/89/112038-09$03.00

have shown that PS–PEP micelles interact strongly at polymer concentrations as low as 1.4% w/w[9]. At a polymer concentration of 10% w/w these micelles exhibit 'crystalline' packing. Hence, the work has shown that even at polymer concentrations below 8% w/w intermicellar interaction effects, which are apparently negligible in PS–PB solutions, do play a significant role in PS–PEP solutions in n-dodecane.

Both the SAXS and SANS investigations have motivated us to find out whether the change of the viscosity of PS–PEP solutions at elevated temperatures can be attributed to changes in the properties of the micelles, e.g. size and intermicellar interaction, rather than to a complete dissociation[3,4]. For this objective, SANS proves particularly advantageous, as it enables direct observation of the structure of the micelles and the interactions between them. This observation may be further facilitated by contrast enhancement via a judicious choice of the deuteration level of the solvent, or even by selective deuteration of the polymer.

Since the drop in the viscosity can also be observed for solutions having a polymer concentration lower than 1.4% w/w (cf. section on 'Experimental materials'), it was first ascertained that the intermicellar interaction exists at 0.5 and 1.0% w/w. For these experiments we used (perdeuterated) n-octane since it was readily available. After having verified that the two solvents are comparable as far as the micellization process is concerned, a 1.0% w/w solution in perdeuterated n-dodecane was used in later experiments to study the effect of temperature on both the intermicellar interaction and the size of the PS–PEP micelles.

EXPERIMENTAL

Materials

The PS-PEP polymer was provided by Dr V. K. Soni from Shell Development Co. (Houston USA) and had been prepared by hydrogenating the polyisoprene block of a polystyrene–polyisoprene diblock copolymer. It had a styrene content of 36.8 ± 1 wt% (according to n.m.r.). Gel permeation chromatography (g.p.c.) measurements in tetrahydrofuran, using polystyrene calibrants, showed that $\bar{M}_w = (1.26 \pm 0.05) \times 10^5$ g mol^{-1} and $\bar{M}_w/\bar{M}_n = 1.07$. The perdeuterated n-octane (>98 mol% D) was obtained from Janssen Chimica, Beerse, Belgium; the perdeuterated n-dodecane (99.4 mol% D) from MSD Isotopes, Montreal, Canada.

To ensure that the polymer dissolved properly, the solutions were heated for 4 h under nitrogen at 80°C (n-octane) and 140°C (n-dodecane).

The viscometry measurements mentioned in the 'Introduction' have shown that the properties of the PS–PEP solutions are dependent on the molecular weights of the two components of the polymer and on the solvent used. It was therefore verified how the polymer–solvent system investigated behaves as a function of temperature.

The effect of temperature on the kinematic viscosity of various solutions of PS–PEP in n-dodecane is shown in *Figure 1*. The decrease in the viscosity at about 90°C is clearly visible for the two highest concentrations. Note that even the 0.5% w/w solution exhibits a detectable viscosity change. Also note the large difference between the viscosities of the 0.5 and 1% w/w solutions at ambient temperature. There is no significant effect of the polymer

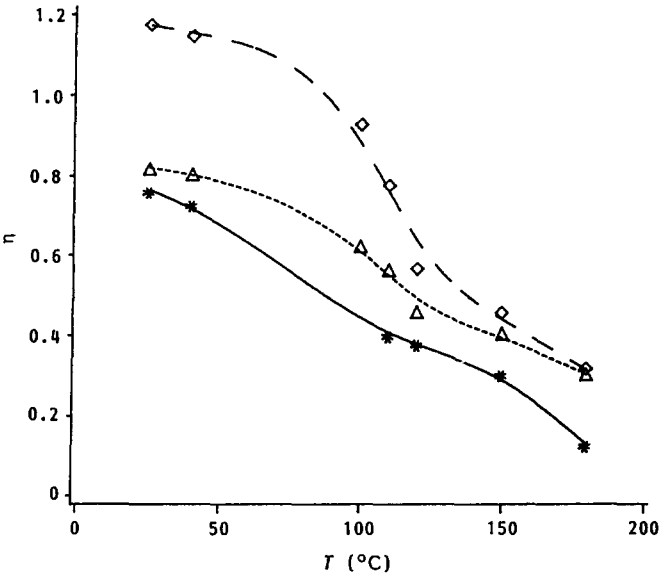

Figure 1 The reduced viscosity of 0.1% (*), 0.5% (△) and 1.0% (◇) w/w PS-PEP solutions in n-dodecane as a function of temperature

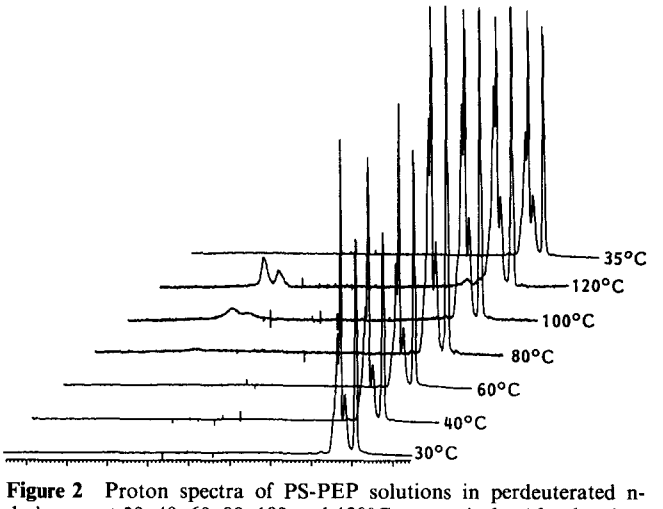

Figure 2 Proton spectra of PS-PEP solutions in perdeuterated n-dodecane at 30, 40, 60, 80, 100 and 120°C, respectively. After heating, the measurement was repeated at 35°C to verify reversibility of the line broadening. Note the appearance of the aromatic proton signal at $\delta \approx 7$ ppm above 80°C, indicative of an increased mobility of the polystyrene blocks

concentration on the temperature at which the viscosity drop occurs.

Figure 2 shows the effect of temperature on the proton n.m.r. line width. The emergence and subsequent narrowing of the aromatic proton signal corresponding to the PS block of the polymer, which is indicative of increasing mobility of the PS block, starts at the same temperature as the onset of the viscosity drop of the solution.

Both the temperature effect on the viscometric behaviour and the line narrowing were found to be reversible.

Small-angle neutron scattering

The experiments were conducted at the 6 m SANS spectrometer of Risø National Laboratory[10]. The instrument is equipped with a large (dia. 57 cm) area-sensitive neutron detector[11]. The sample-to-detector distance was 3 m.

For quasi-elastic scattering, the scattering angle 2θ is converted to the scattering vector $\boldsymbol{Q}$, with length $Q=|\boldsymbol{Q}|=4\pi(\sin\theta)/\lambda$. Two wavelengths λ were employed: $\lambda=0.34\,\text{nm}$ to observe the scattering in the Q region where the particle form factor $F(Q)$ deviates from unity significantly, and $\lambda=2.26\,\text{nm}$ to study the structure factor $S(Q)$. The complete Q region investigated extended from 0.025 to $1.5\,\text{nm}^{-1}$. The full-width at half-maximum (FWHM) of the wavelength distribution was $\Delta\lambda/\lambda=0.2$.

The solutions were contained in sealed quartz cuvettes (dia. 10 mm) with a neutron flight path of 1 mm. For the measurements at ambient temperatures an automatic six-position sample changer was available. However, only a single specimen could be placed in the furnace. The sample temperature was verified to be stable within 0.5°C during the course of the measurement, and its inaccuracy did not exceed 1°C. The temperature was increased sufficiently slowly to prevent overshooting. At the desired temperature, the solution was equilibrated for 15 min prior to the start of the measurement. Ample volume was left in the cuvettes for the solution to expand during heating.

The scattering intensity I in each detector element, after subtraction of the blank (i.e. background, solvent and cuvette) scattering I_b, was normalized to the incoherent scattering of lupolene I_L:

$$I_S=(I-I_b)/I_L$$

As the resultant scattering was isotropic for all the concentrations investigated, it was subsequently radially averaged with respect to the position of the primary beam to obtain the scattering $I(Q)$ vs. scattering vector Q.

For the measurements at elevated temperatures, the blank scatterer was kept at 25°C. In principle this introduces a systematic error, which, however, is not considered serious for the subsequent analysis.

THEORY

The theory of SANS is well described in various textbooks[12]. Here only the aspects necessary for the interpretation of the present data have been retained. Our interpretation is focused on the dimensions of and interactions between the micelles in order to investigate the thermal stability of the micelles. The scattering intensity $I(Q)$ for a particulate system with random orientations can be expressed, apart from an instrumental proportionality constant, as:

$$I(Q)=N_pV_p^2(\Delta\rho)^2F^2(Q)S(Q) \qquad (1)$$

In this equation, N_p and V_p are the number density and the volume of the particles, respectively, and $(\Delta\rho)^2$ is the scattering contrast. The values of this quantity pertinent to the present investigation are listed in *Table 1*. $F(Q)$ is the single-particle form factor describing the form and the dimensions of the particles and can often be treated in the Guinier approximation:

$$F^2(Q)\propto\exp(-Q^2R_g^2/3)$$

with R_g the 'Guinier radius' or radius of gyration. For spherical particles of radius R_s the following holds: $R_s=(\sqrt{5}/3)R_g$. In (1), $S(Q)$ is the structure factor or the interparticle interference factor, which differs from 1 for interacting particles only. We have assumed that the micelles have a monodisperse size distribution, which is confirmed by g.p.c. and ultracentrifuge studies.

Table 1 Contrast factors $(\Delta\rho)^2$ (in units $10^{28}\,\text{m}^{-4}$) for a number of materials pertinent to this investigation

Polystyrene	Protonated n-octane	2.96
Polystyrene	Perdeuterated n-octane	27.2
Poly(ethylene/propylene)	Protonated n-octane	0.01
Poly(ethylene/propylene)	Perdeuterated n-octane	46.5
Polystyrene	Poly(ethylene/propylene)	2.56

According to equation (1), both $S(Q)$ and $F(Q)$ contribute to $I(Q)$. However, $S(Q)$ and $F(Q)$ have different Q dependences, which makes it possible in our case to separate their contributions to $I(Q)$. As may be concluded from the scattering data, for the region $Q<0.1\,\text{nm}^{-1}$, the influence of the structure function is relatively large, whereas for large Q values $S(Q)\to1$. The scattering at $Q>0.2\,\text{nm}^{-1}$ is dominated by $F(Q)$. In our case Guinier behaviour was observed in the region between $Q=0.2$ and $0.5\,\text{nm}^{-1}$, i.e. a plot of $\ln(I)$ *versus* Q^2 gives a straight line. The slopes of such lines were then used to calculate the Guinier radii of the particles.

The region above $Q=0.2\,\text{nm}^{-1}$ can also be used for the calculation of the distance distribution function $p(r)$[13]. For a dilute solution of particles, the scattering $I(Q)$ is given by:

$$I(Q)=\int_0^\infty dr\,p(r)\,(\sin Qr)/Qr \qquad (2)$$

In this equation, prefactors comprising the contrast and the number of scattering centres have been omitted for clarity; $p(r)\,dr$ is proportional to the number of distances within the particle of length between r and $r+dr$. Since $p(r)$ and $I(Q)$ form Fourier pairs, the maximum information concerning the micelle is contained in $p(r)$. For the present analysis, an inversion scheme of equation (2) as developed by Moore[14] is employed. For spherical particles the distribution $p(r)$ is given by:

$$p(r)=12x^2(2-3x+x^3),\qquad x=r/2R \qquad (3)$$

where R stands for the radius of the particle. Information extracted from $p(r)$ can be used to verify further the validity of the Guinier approximation. In this way an internal check on our interpretation of the data has been obtained.

RESULTS

Room-temperature measurements

Solutions of PS–PEP diblock copolymer in perdeuterated n-octane (0.5%, 1% and 2% w/w) and in protonated n-octane (0.25% and 1% w/w) were studied. A 1% w/w solution in perdeuterated n-dodecane was further investigated at various temperatures. The small-angle scattering from these solutions is remarkably rich in details. Three regions in Q space need to be distinguished:

(i) For $Q<0.1\,\text{nm}^{-1}$, a broad maximum in the scattering is observed. This maximum is both too intense and at too small a scattering angle to be a feature of the micelle form factor $F(Q)$. Hence this peak evidences, even at these low polymer concentrations, the occurrence of interparticle interferences.

(ii) For $0.2\,\text{nm}^{-1}<Q<0.5\,\text{nm}^{-1}$, Guinier behaviour is observed directly leading to estimates for the size of the micelles.

(iii) For $Q>0.6\,\text{nm}^{-1}$, very weak maxima in the

scattering intensity occur, undoubtedly related to the particle form factor.

In order to separate the form factor contribution to $I(Q)$ in the Q region below 0.1 nm^{-1}, $F(Q)$ was determined in the second region ($0.2\,nm^{-1} < Q < 0.5\,nm^{-1}$) first. The plot of $\ln(I)$ *versus* Q^2 yields a straight line in this region, resulting in Guinier radii $R_g = 8.4 \pm 0.2$ and $R_g = 9.5 \pm 0.5$ nm for protonated and perdeuterated n-octane solvent, respectively (the given precision is based on counting statistics). It should be kept in mind that these values constitute volume-weighted averages over both the PS core and the PEP domains. The contrast between the PEP blocks and the protonated octane (cf. *Table 1*), however, is negligible, which means that the Guinier radius in protonated octane directly yields the radius of the polystyrene core: $R_c = 10.8$ nm. In the deuterated octane the PEP blocks contribute to the Guinier radius, but now the particle should be considered as a composite particle. For such particles the Guinier radius is weakly dependent on the contrast[15]:

$$R_g^2 = R_{gM}^2 + \frac{1}{\Delta\rho V_p} \int dr\, r^2 \rho_F(r) \qquad (4)$$

where

$$R_{gM} = \left[(1/V) \int dr\, r^2 \right]^{1/2}$$

is the mechanical radius of gyration at infinite contrast ($1/\Delta\rho \to 0$), and $\rho_F(r)$ constitutes a fluctuation contribution to the scattering-length density inside the particle.

When we assume that the PS core is surrounded by a homogeneous concentric layer of PEP arms, the contrast variation method[15,16] can be applied to determine $1/\Delta\rho$ and $\bar{\rho}$, the average scattering length density. A rough estimate based on only two data points results in a total particle size of 9.4 nm. The model of homogeneous concentric layers, however, deviates from the more probable model of PEP arms protruding from the PS core into the solution. Therefore the 9.3 nm is only a very rough estimate. *Table 2* summarizes results for micelle form factor parameters based on various methods.

A nice check on the measured Guinier radius is provided by the distance distribution function $p(r)$. The result of the calculation as based on the calculation method developed by Moore is shown in *Figure 3*. Except for a small bulge at larger distances, $p(r)$ for the micelles in protonated octane closely resembles the spherical-particle expression as given in equation (3).

Table 2 Determination of the micelle form factor parameters based on various methods. Within the uncertainty, these numbers are valid for the 0.5%, 1.0% and 2.0% w/w solutions in perdeuterated n-octane (D-octane) and protonated n-octane (H-octane)

Method	R_g (nm)	R_{tot} (nm)	R_c (nm)	D_{max} (nm)
Guinier adjustment				
H-octane	8.4±0.2	–	10.8±0.3	–
D-octane	9.5±0.5	–		–
Contrast variation	7.2	9.3	–	–
Secondary maxima in $F^2(Q)$	–	–	9.0	–
$p(r)$				
H-octane	–	–	10.5	23.0
D-octane	9.4±0.2	–		

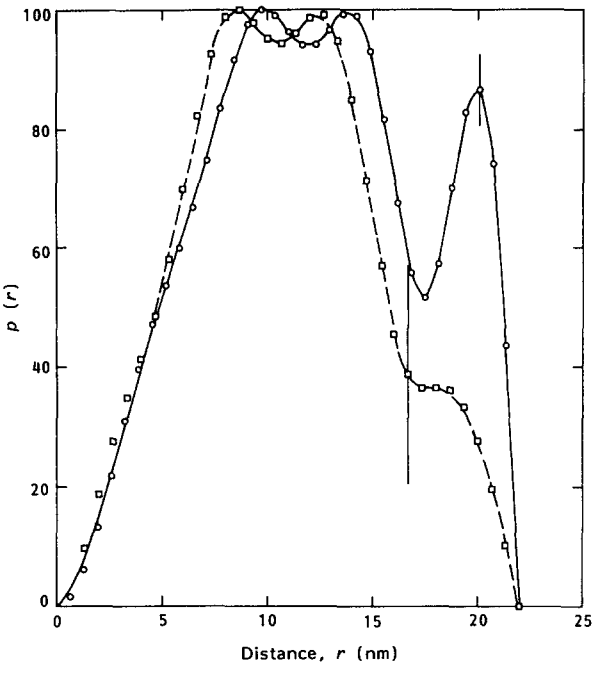

Figure 3 Distance distribution function $p(r)$ for a 1% w/w PS-PEP solution in protonated (□) and perdeuterated (○) n-octane. The vertical bars illustrate the accuracy of $p(r)$

The bulge in $p(r)$ near a distance of 20 nm indicates that a small contrast remains between the solvent and the PEP domain. The dip in $p(r)$ about $r = 10$ nm is presumably an artefact of the calculation method. For the perdeuterated solvent, the contrast with the PEP domain is more than 1000 times larger, leading to a significant increase in the number of large distances in $p(r)$. Note that for both solvents the $p(r)$ function exhibits a cut-off at $D_{max} = 23$ nm, which defines the maximum size of that part of the micelle that is detectable by the neutron. In a next step not effected here, $p(r)$ could be used in further modelling the particle[17]. A determination of the Guinier radius based on the distance distribution function $p(r)$ yields a slightly more accurate value than the Guinier parameter adjustment: $R_g = 9.4 \pm 0.2$ nm, as opposed to $R_g = 9.5 \pm 0.5$ nm with the latter method.

The agreement between the particle size obtained with the Guinier approximation and with $p(r)$ indicates that the Q region between 0.2 and 0.5 nm^{-1} can be used to find the contribution of $F(Q)$ in the small-Q region for $Q < 0.2\,nm^{-1}$.

The scattering region at very low Q ($Q < 0.1\,nm^{-1}$) is given in *Figure 4*. Quite surprisingly, even at a concentration as low as 0.5 wt%, some interparticle interference is present. Clearly, for increasing concentration, the peaks in the scattering shift to higher scattering angles, indicating a smaller centre-to-centre separation distance D_{sep} of the micelles. The peak intensities do not exactly scale with the particle number density; the discrepancy, however, is small. In *Figure 4* the tail of the scattering, dominated by the form factor, can be used to determine the intensity prefactor in equation (1). After dividing the scattering curve by this prefactor and $F^2(Q)$, the interparticle interference function is retrieved (*Figure 5*). The peak positions in $S(Q)$ at Q_{max} may be converted to D_{sep} by applying:

$$D_{sep} \approx 2\pi/Q_{max} \qquad (5)$$

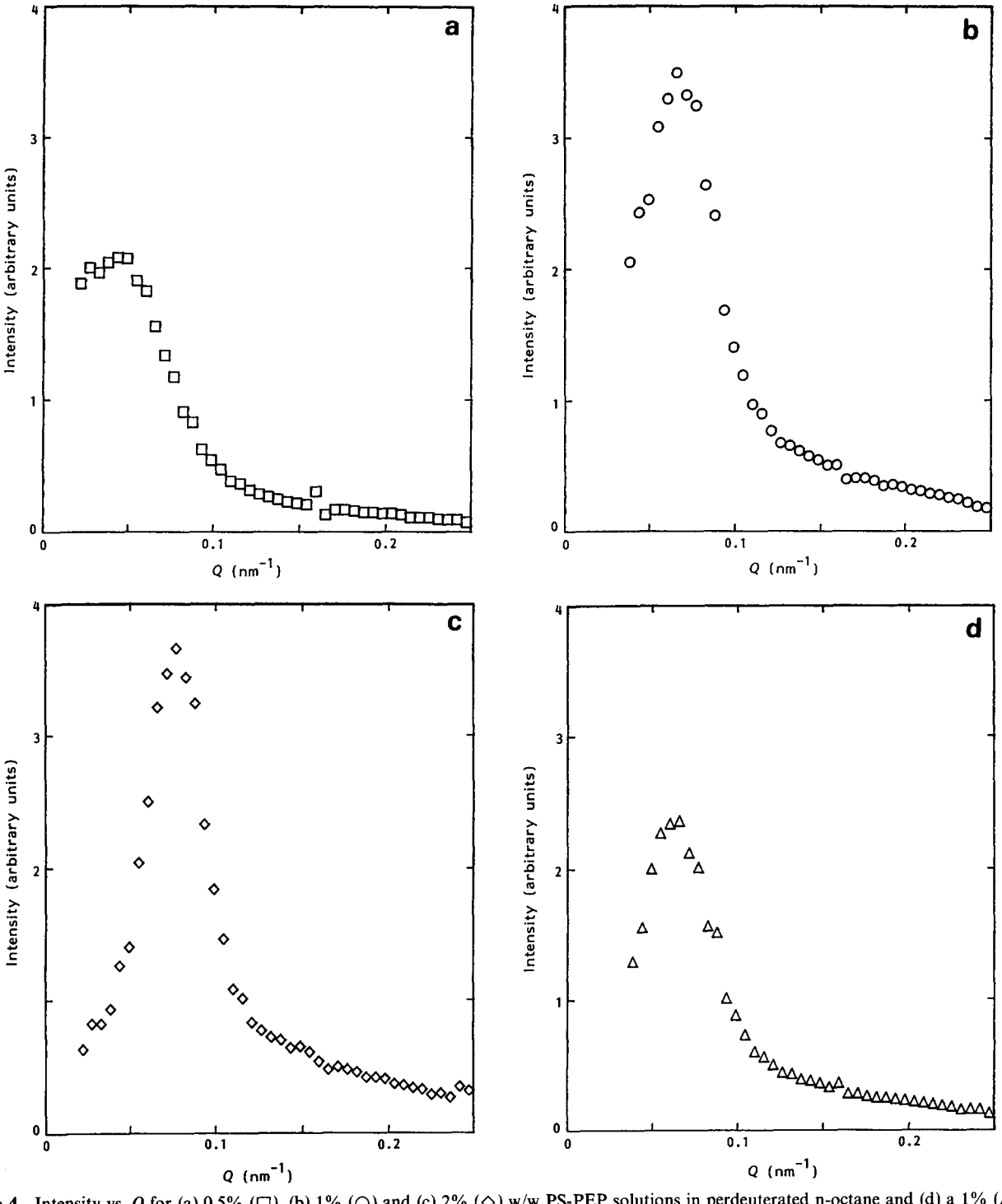

Figure 4 Intensity vs. Q for (a) 0.5% (□), (b) 1% (○) and (c) 2% (◇) w/w PS-PEP solutions in perdeuterated n-octane and (d) a 1% (△) w/w solution in perdeuterated n-dodecane for very low Q ($Q<0.2\,nm^{-1}$) at 25°C

D_{sep} calculated by equation (5) is equal to d given by Bragg's law for diffraction in a crystal. Since here the maximum is caused by a diffraction phenomenon in liquid-type ordered material, D_{sep} is underestimated by 20%[12]. As expected, D_{sep} increases with decreasing polymer concentration: 90 nm, 100 nm and 160 nm for the 2%, 1% and 0.5% w/w solutions, respectively. However, D_{sep} is not proportional to the cubic root of the polymer weight fraction, Φ_w, indicating that, although the number of micelles is small, the solutions are not dilute in the ordinary sense. For dense solutions ($\Phi_w>2.0\%$ w/w), the interparticle distance approaches 90 nm. With due consideration of the size of the micelle core, this figure sets a lower limit to the thickness of the PEP domain surrounding the core of about 70 nm. Since the contour length of a PEP chain is of the order of 400 nm, this suggests that the PEP chains of neighbouring micelles overlap. Dynamic light scattering measurements, which we carried out recently, corroborate this. For PS–PEP micelles a hydrodynamic radius of approximately 50 nm was found.

We now turn to the region for $Q>0.5\,nm^{-1}$. *Figures 6a* and *6b* present exploded views for $Q>0.4\,nm^{-1}$ for the protonated octane. In both cases, one distinct maximum at $Q=1.0\,nm^{-1}$ is visible, while there is a less pronounced maximum at $Q=0.6\,nm^{-1}$. These features

indicate secondary maxima, implying that the micellar cores are spherical and that the size distribution is very narrow. In *Figure 6c* the maxima for a deuterated solution are much less prominent. This may indicate that the PEP shell has less well defined spherical symmetry.

The position of the secondary maxima for spherical particles depends on the radius R. At the first maximum $QR = 5.8$, while at the second maximum $QR = 9.1$. From the position of these maxima at a Q of roughly 0.6 and 1.0 nm^{-1}, a core radius of about 9 nm can be deduced, which is in fair agreement with the other data. It should be mentioned that the first maximum should have a higher intensity than the second maximum, which is, probably as a result of poor counting statistics, not the case for the protonated octane.

Heat treatment

We finally discuss the behaviour of the micelles on heat treatment. The 1% w/w solution in perdeuterated n-dodecane was subjected to temperatures between 25 and 160°C (the boiling point of n-dodecane is 216°C). Although the number of data points in the Guinier region ($0.2\,nm^{-1} < Q < 0.5\,nm^{-1}$) is limited, determinations of R_g are consistent with those of other methods (cf. previous subsection). When the solution is heated, R_g first increases

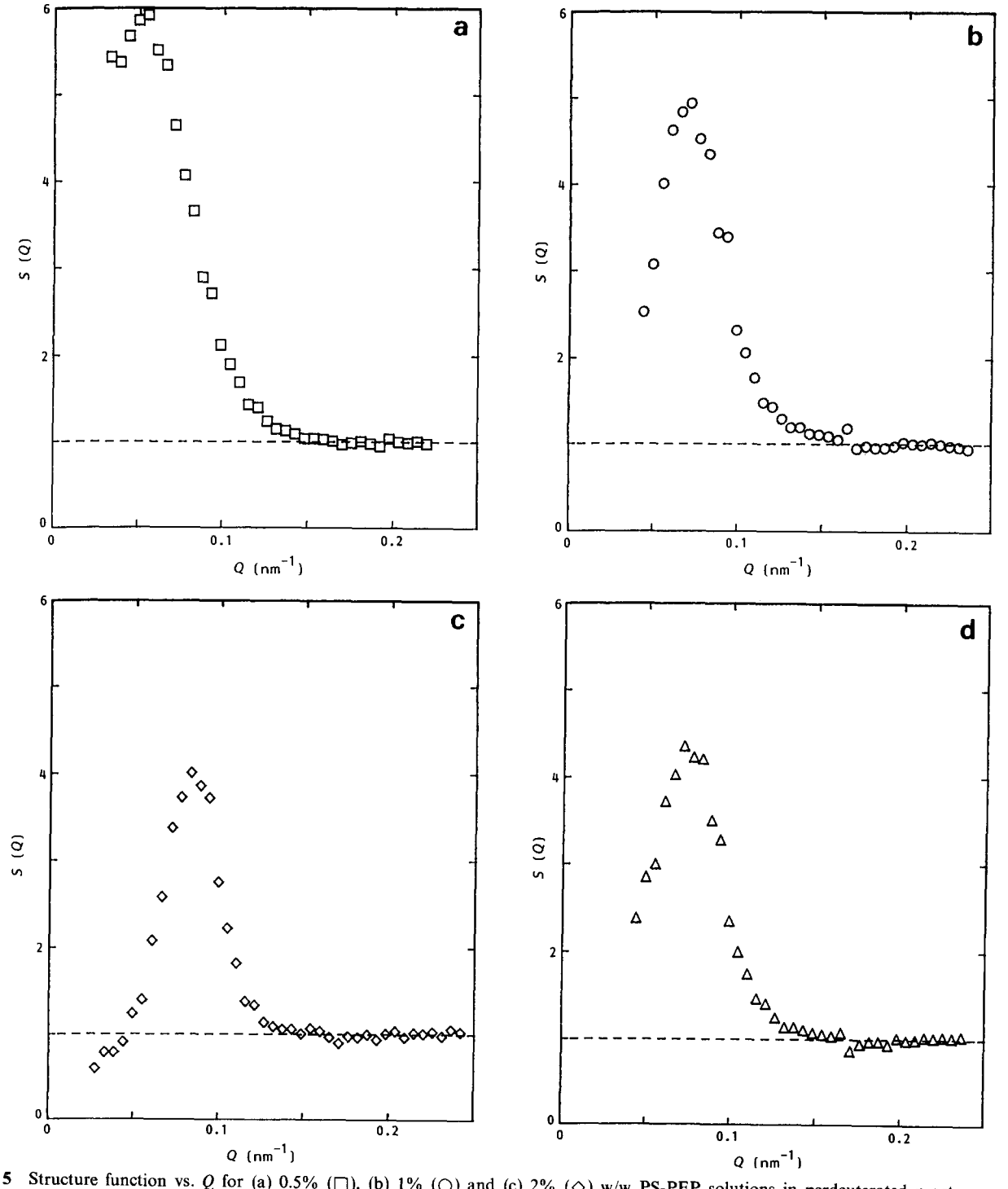

Figure 5 Structure function vs. Q for (a) 0.5% (□), (b) 1% (○) and (c) 2% (◇) w/w PS-PEP solutions in perdeuterated n-octane and (d) a 1% (△) w/w solution in perdeuterated n-dodecane for very low Q ($Q < 0.2\,nm^{-1}$) at 25°C

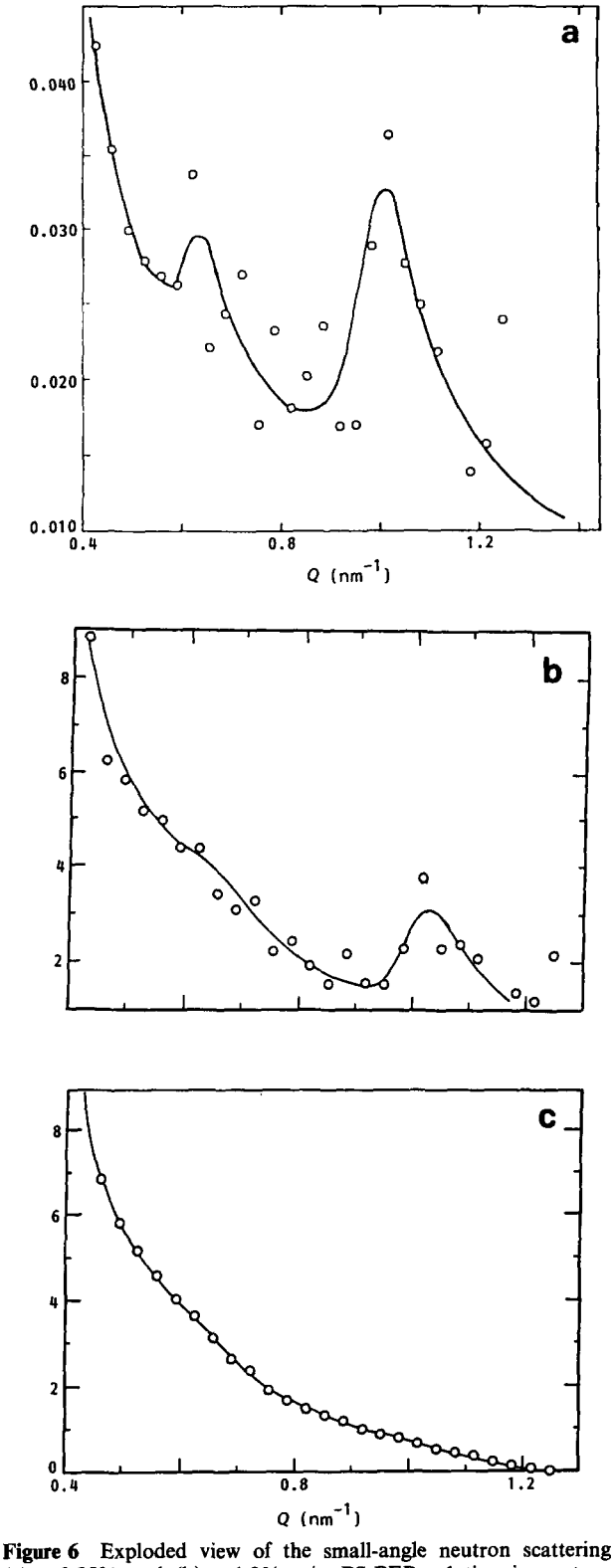

Figure 6 Exploded view of the small-angle neutron scattering of (a) a 0.25% and (b) a 1.0% w/w PS-PEP solution in protonated n-octane, and (c) a 1% w/w solution in perdeuterated n-octane

slightly, followed by a remarkable drop above 100°C. Simultaneously, the scattering intensity, exhibiting no marked temperature dependence up to 80°C, drops, until at 160°C it is only 10% of its maximum value. These dramatic changes are most conspicuous in *Figure 7*. Before drawing firm conclusions, first, by careful analysis, the temperature dependences of the solvent and the solute have to be separated. By taking account of the temperature dependence of the mass density $n_m(T)$ of perdeuterated n-dodecane, the scattering-length density $\rho_m(T)$ of the solvent can be calculated in the pertinent temperature range. As the temperature increases, the scattering contrast between the micelle and the solvent decreases, owing to the decreased solvent density. This would invoke an apparent increase of R_g not related to any real volume change of the micelle itself. However, inspection of equation (4) reveals that the contrast dependence of R_g for the present system is so weak that any such temperature effect will escape observation (cf. the broken curve in *Figure 7*). The observed changes in R_g thus reflect an expansion and subsequent shrinking of the micelle core upon heating.

The temperature dependence of the scattering intensity is more difficult to analyse. According to equation (1), three factors contribute to the intensity prefactor. Of these, the temperature dependence of the contrast $(\Delta\rho)^2$ can be tracked with the known $n_m(T)$. The increased specific volume of the solvent at elevated temperature will result in an apparent decrease of the particle number density N_p. This decrease with temperature can be calculated in a similar manner to $(\Delta\rho)^2(T)$. Finally, volume changes of the micelle may lead to dramatic changes in the scattering intensities. Since $I \propto V_p^2 \propto R_g^6$, changes in R_g will be magnified enormously in the scattering intensity. All these effects lead to an anticipated temperature dependence of the intensity as shown by the chain curve in *Figure 7*. Indeed, the dramatic reduction in intensity for temperatures above 100°C is largely due to the decreased micelle size. The agreement between this

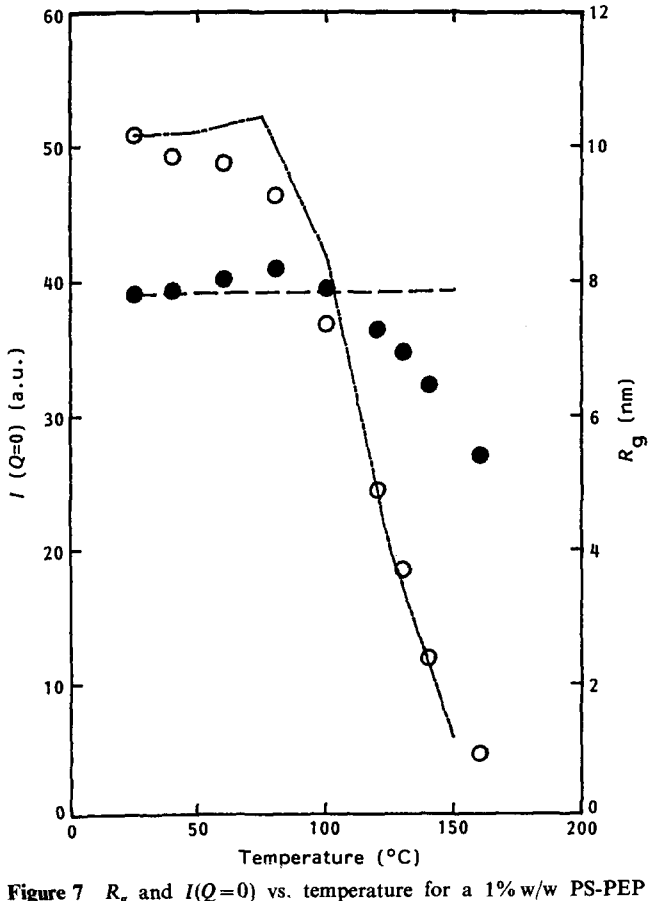

Figure 7 R_g and $I(Q=0)$ vs. temperature for a 1% w/w PS-PEP solution in perdeuterated n-dodecane. The broken curve represents the temperature dependence of R_g if the particle remains the same size. The chain curve represents the calculated temperature dependence of the zero angle scattering, comprising all effects discussed in the text

curve and the data, especially at higher temperatures, is gratifying. A particular point of interest here is that no further assumptions are necessary to describe satisfactorily the temperature dependence of the intensity, i.e. the number of aggregates in the solution remains the same.

It should be noted here that the temperature will also affect the scattering-length density $\bar{\rho}$ of the micelle. For composite particles for which the contributions of the various phases to the volume-averaged $\bar{\rho}$ are not known *a priori*, it is barely possible to quantify this dependence. For the particles at hand, estimates indicate that this effect is not negligible, but does not exceed 10% of the effects already discussed within the investigated temperature range. Therefore, instead of trying to modify $\bar{\rho}(T)$ in an unreliable way, $\bar{\rho}$ is kept constant in the calculation, but this intractable temperature dependence is added to the uncertainty. Any ambiguity concerning R_{gM} at elevated temperatures may, of course, be eliminated by application of the contrast-variation technique.

The present findings are corroborated by a small shift to lower angles of the form factor maxima (cf. *Figure 6*) for temperatures up to 100°C. This shift is indicative of a small increase of the micelle size. Above 100°C the secondary maxima in $F^2(Q)$ are no longer discernible, suggesting that the micelle contraction is not uniform for all aggregates.

The investigation of the structure factor $S(Q)$ at elevated temperatures is hampered by a lack of a good blank correction. Nevertheless, the most prominent feature in *Figure 8* is that at 140°C considerable micelle interference effects are still discernible, confirming the presence of the aggregates. The intensity drop of this peak upon heating from 100 to 140°C exceeds the corresponding intensity drop in the Guinier region of the scattering by about 50%. Simultaneously, the FWHM of the peak has increased when the temperature is raised from 100 to 140°C. Both effects indicate that in the rise from 100 to 140°C the intermicellar interaction is reduced dramatically.

Finally, during cooling after these experiments were concluded, it was verified at some selected temperatures that the heat treatment of the solutions is reversible.

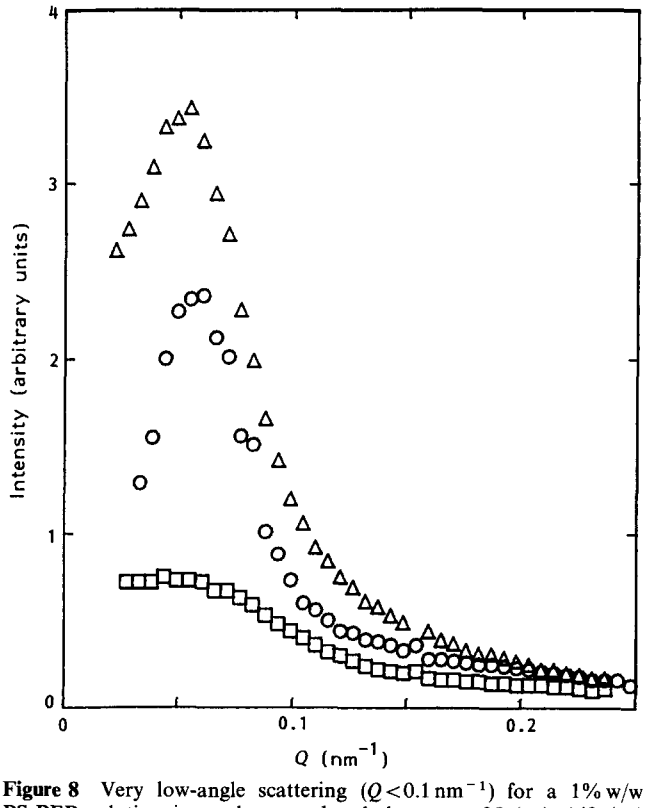

Figure 8 Very low-angle scattering ($Q<0.1\,nm^{-1}$) for a 1% w/w PS-PEP solution in perdeuterated n-dodecane at 25 (○), 140 (□) and 100°C (△) (after cooling from 160°C). Note that, owing to incomplete blank scattering correction, absolute intensity comparisons are meaningless

DISCUSSION

The present SANS results show that, in the concentration range between 0.5 and 2% w/w, intermicellular interference results in a 'liquid-like' ordering of the micelles in the solution (at 6% w/w Higgins *et al.*[9] even observed 'crystal-like' ordering). This strong interference effect probably accounts for the high thickening power of PS-PEP polymer in an aliphatic solvent. However, as was mentioned in the introduction, the purpose of this study has been to investigate whether the drop in the viscosity of the PS-PEP solutions in n-dodecane, which sets in at approximately 80°C, is caused by dissociation of the micelles into single polymer molecules.

Quite surprisingly, this seems not to be the case. When the temperature in the SANS experiment is increased, the micellar core, after a slight swelling between 80 and 100°C, starts to shrink from 100°C onwards. At 160°C the core radius has been reduced by 30%. This reduction of the core radius is consistent with the observed decrease in the total scattering intensity as expected on the basis of equation (1). Apparently, the aggregation number of the micelles starts to decrease above 100°C, resulting in smaller micellar cores, but the total number of micelles does not change notably. Hence, according to SANS, micellar dissociation does not take place over a narrow temperature trajectory, but is rather smeared out between roughly 100°C and a temperature above 160°C. It is not obvious how this gradual dissociation process of the micelles would be able to cause a sharp viscosity drop over a 30°C span. Moreover, the viscosity drop sets in at 80°C, where the micelles even swell slightly instead of decreasing in size. This suggests that a micellar property other than the micellar dimension or aggregation number is important.

Knowing that the intermicellar interference has a large influence on the solution viscosity, a closer look at the shape and position of the structure peak is necessary. Unfortunately, we carried out low-Q measurements at three different temperatures only. However, the limited data we have obtained so far indicate that above 100°C the intermicellar interference diminishes rapidly, as can be inferred from the broadened scattering maximum at low Q at 140°C. Between 25 and 100°C no significant changes in the intermicellar interaction seem to have occurred. A further point of interest is that no appreciable shift in the peak maximum is found (after correction for the thermal expansion of the solution), which implies that the average intermicellar separation distance is independent of temperatures up to 140°C. This is additional evidence that at least a major part, if not all, of the micelles still exists at 140°C. Clearly, if most of the micelles had disappeared at 140°C, the peak would either have disappeared completely, or, if some residual ordering had been detectable, the peak would have shifted

to lower Q values as a result of the increased intermicellar distance. The fact that the structure peak, although broadened, appears roughly at the same Q value as the peaks at 25 and 100°C supports our conclusion that at least the majority of the micelles are still present.

At this moment we explain our observations as follows. We assume that at low (e.g. ambient) temperatures exchange of PS-PEP chains between the micelles and the bulk solution cannot take place because of the glassy state of the PS core material. In this situation, the PEP arms protruding from the micellar core surface are firmly attached to that surface. When a force is exerted on a PEP arm, such as a pulling force caused by an entanglement with a (moving) neighbouring micelle, the motions of both micelles to which the entangled PEP arms are attached will be affected. The two micelles will behave as rigid particles covered with firmly attached polymer chains. Hence, the overlap between PEP coronas of neighbouring micelles (and the resultant entanglements between their PEP chains) will result in strong intermicellar interference effects.

However, when the micellar solutions are heated above a temperature, T_p, at which the core material becomes soft and plastic, the higher mobility of the PS blocks in the core of the micelle allows a dynamic equilibrium between micelles and free PS–PEP chains to be established. When the temperature is steadily increased, the core plasticity increases further and the exchange rate between micelles and the bulk will increase. At the higher temperatures the increased solubility of the PS segments will shift the equilibrium towards the free chains. According to our SANS measurements this is achieved by lowering the aggregation number of the micelles. In that case the number of arms per micelle will be reduced when the temperature is increased. Clearly, fewer PEP arms per micelle result in a reduction of the number of entanglements between neighbouring micelles and consequently less intermicellar interactions.

Probably more important is the fact that, at temperatures above T_p, the PS–PEP chains are no longer firmly attached to the micelles, but can exchange rapidly with the bulk solution. Especially in flow fields, where the strains on a micelle, surrounded by a moving array of neighbouring micelles, are high, the fact that complete chains can be drawn out quite easily will facilitate flow considerably. Both effects, viz. the reduction of the micellar aggregation number and the increased core plasticity, will greatly reduce the thickening power of the polymer above T_p.

It is known that the exchange between PS–PEP micelles and free chains is negligibly slow at low temperatures. Price *et al.* have shown that PS–PEP micelles are able to pass a g.p.c. column without difficulty at 50°C (ref. 18). Above 75°C, however, experiments fail due to adsorption of PS blocks of the polymer onto the column material. Apparently, at a temperature between 50 and 75°C, the PS blocks become exposed to the gel of the column, probably because then the exchange between free chains and micelles has become rapid on the timescale of the g.p.c. experiments (typically several hours). The existence of a transition temperature at which exchange with the bulk sets in is further corroborated by the n.m.r. experiments mentioned in the 'Introduction'. The narrowing of the aromatic proton signal becomes observable at approximately 80°C. The narrowing process continues gradually up to 135°C and reflects the increasing rate of exchange between the micellar and free chain states and the gradual shift to the free chain state.

With SANS no evidence for a sharp dissociation temperature of the micelles has been observed up to 160°C. Based on experimental results obtained thus far we conclude that the sudden change of the viscosity of PS–PEP solutions near 80°C is caused by changes in the properties of the micellar core, resulting in a dynamic equilibrium between PS–PEP chains in the micellar and free chain state.

ACKNOWLEDGEMENTS

The authors are grateful for helpful discussions with Drs J. S. Higgins, J. K. Kjems, C. van Dijk and J. K. Arnette.

REFERENCES

1 Price, C., Hudd, A. L., Stubbersfield, R. B. and Wright, B. *Polymer* 1980, **21**, 9
2 Tuzar, Z. and Kratochvil, P. *Adv. Colloid Interface Sci.* 1976, **6**, 201
3 Mandema, W., Zeldenrust, H. and Emeis, C. A. *Makromol. Chem.* 1979, **180**, 1521
4 Mandema, W., Zeldenrust, H. and Emeis, C. A. *Makromol. Chem.* 1979, **180**, 2163
5 Candau, F., Heatley, F., Price, C. and Stubbersfield, R. B. *Eur. Polym. J.* 1984, **20**(7), 685
6 Watanabe, H., Kotaka, T., Hashimoto, T., Shibayama, M. and Kawai, H. *J. Rheol.* 1982, **26**(2), 153
7 Shibayama, M., Hashimoto, T. and Kawai, H. *Macromolecules* 1983, **16**, 16
8 Hashimoto, T., Shibayama, M., Kawai, H., Watanabe, H. and Kotaka, T. *Macromolecules* 1983, **16**, 361
9 Higgins, J. S., Dawkins, J. V., Maghami, G. G. and Shakir, S. A. *Polymer* 1986, **27**, 931
10 Kjems, J. K., Bauer, R., Christensen, P., Freltoft, T., Nielsen, L. G. and Linderholm, J. 'Neutron Scattering in the Nineties', International Atomic Energy Agency, Vienna, IAEA-CN-46, 1985, p. 495
11 Kjems, J. K., Bauer, R., Breiting, B. and Thuesen, A. 'Neutron Scattering in the Nineties', International Atomic Energy Agency, Vienna, IAEA-CN-46, 1985, p. 489
12 Bacon, G. E. 'Neutron Diffraction', Clarendon Press, Oxford, 1967
13 Glatter, O. *J. Appl. Crystallogr.* 1977, **10**, 415
14 Moore, P. B. *J. Appl. Crystallogr.* 1980, **13**, 168
15 Jacrot, B. *Rep. Prog. Phys.* 1976, **39**, 911
16 Markovic, I., Ottewill, R. H., Cebula, D. J., Field, I. and Marsh, J. F. *Colloid Polym. Sci.* 1984, **262**, 648
17 Glatter, O. 'Small-Angle X-ray Scattering' (Eds O. Glatter and O. Kratky), Academic Press, London, 1982, Ch. 5
18 Price, C., Hudd, A. L., Booth, C. and Wright, B. *Polymer* 1982, **23**, 650